Physics and Chemistry of the Earth 83–84 (2015) 57–64

Contents lists available at ScienceDirect

Physics and Chemistry of the Earth

journal homepage: www.elsevier.com/locate/pce

A temperature-dependent multi-relaxation spectroscopic dielectric model for thawed and frozen organic soil at 0.05–15 GHz

Valery Mironov *, Igor Savin

Kirensky Institute of Physics, Akademgorodok 50/38, 660036 Krasnoyarsk, Russia

ARTICLE INFO

Article history:
Received 31 October 2014
Received in revised form 24 February 2015
Accepted 26 February 2015
Available online 14 March 2015

Keywords:
Organic soil
Moisture
Temperature
Dielectric model
Thawed and frozen soil
SMOS

ABSTRACT

A dielectric model for thawed and frozen Arctic organic-rich soil (50% organic matter) has been developed. The model is based on soil dielectric measurements that were collected over ranges of gravimetric moisture from 0.03 to 0.55 g/g, dry soil density from 0.72 to 0.87 g/cm^3, and temperature from 25 to −30 °C (cooling run) in the frequency range of 0.05–15 GHz. The refractive mixing dielectric model was applied with the Debye multi-relaxation equations to fit the measurements of the soil's complex dielectric constant as a function of soil moisture and wave frequency. The spectroscopic parameters of the dielectric relaxations for the bound, transient bound, and unbound soil water components were derived and were complimented by the thermodynamic parameters to obtain a complete set of parameters for the proposed temperature-dependent multi-relaxation spectroscopic dielectric model for moist soils. To calculate the complex dielectric constant of the soil, the following input variables must be assigned: (1) density of dry soil, (2) gravimetric moisture, (3) wave frequency, and (4) temperature. The error of the dielectric model was evaluated and yielded RMSE$_{\varepsilon'}$ values of 0.348 and 0.188 for the soil dielectric constant and the loss factor, respectively. These values are on the order of the dielectric measurement error itself. The proposed dielectric model can be applied in active and passive microwave remote sensing techniques to develop algorithms for retrieving the soil moisture and the freeze/thaw state of organic-rich topsoil in the Arctic regions.

1. Introduction

The most promising results in the remote sensing of soil moisture, freeze/thaw state, and temperature over land surfaces have been obtained using microwave radiometry and radar techniques. Contemporary space missions using these techniques, such as AQUA, GCOM-W (Global Change Observation Mission), SMOS (Soil Moisture and Ocean Salinity), SMAP (Soil Moisture Active Passive), RADARSAT (Radar Satellite), and ALOS PALSAR (Advanced Land Observing Satellite Phased Array type L-band Synthetic Aperture Radar), employ radiometers and radars that function in the frequency range from 1.2 GHz to 89 GHz. Dielectric models of topsoil are a crucial element of retrieval algorithms that are used to obtain geophysical characteristics of the land surface, such as soil moisture, temperature, and freeze/thaw state, with these techniques.

Recent research in microwave radiometry and radar remote sensing has been focused on the Arctic region (Bircher et al., 2012; Jones et al., 2007; Mironov et al., 2013a; Rautiainen et al., 2012; Watanabe et al., 2012). The topsoil in both boreal forests and Arctic tundra generally contains organic-rich soils, which requires that dielectric models for these soils be available to develop retrieval algorithms. A dielectric model for the organic-rich Arctic soil in the area of North Slope, Alaska, was proposed by Mironov et al. (2010a). This model provides predictions of the complex dielectric constant (CDC) for one type of thawed and frozen organic-rich soil as a function of frequency, temperature, and moisture ranging from 1.0 to 16 GHz, 25 to −30 °C, and 0.05 to 1.1 g/g, respectively. The CDC of moist soil depends on the type of solids in the soil. Therefore, to develop remote sensing algorithms for natural environments, the dielectric models for other organic soils are needed.

This paper presents measurements of an organic-rich soil sample that was collected on the Yamal Peninsula and develops a temperature-dependent multi-relaxation spectroscopic dielectric model (TD MRSDM). Compared to the model in Mironov et al. (2010a), the frequency range was extended from 1–16 GHz to 0.05–15 GHz, and many additional dielectric relaxations of soil water were detected in the frequency range of 0.05–1.0 GHz. As a result, a new approach to processing the measured dielectric data was applied, and the theoretical dielectric model of moist soil used in Mironov et al. (2010a) was modified to address the multi-relaxation characteristics of the measured dielectric data of the soil

* Corresponding author. Tel./fax: +7 3912905028.
E-mail address: rsdvm@ksc.krasn.ru (V. Mironov).

http://dx.doi.org/10.1016/j.pce.2015.02.011
1474-7065/

samples as was done in Mironov et al. (2013b) for thawed mineral soils. The temperature range for the frozen soil samples was also substantially extended from −30 °C to −7 °C (as in Mironov et al., 2010a) to −30 °C to −1 °C, which allowed taking into account the intensive phase transitions of soil water between −1 °C and −7 °C that were observed in a cooling run.

2. Soil samples and measurement procedures

The soil sample that was analyzed was collected during fieldwork conducted at a typical grassy moss tundra site located at N70°25′52″, E68°25′19″ at an elevation of 39.3 m. The sample was extracted from depths between 9 and 14 cm and consists of mineral solids and decomposed organic matter. In vivo, the air dry bulk density of the sample is 0.26 g/cm^3. The percentages of organic matter and mineral solids are as follows: organic matter ~50%, quartz ~30%, potassium feldspar ~5–10%, plagioclase ~5–10%, and chlorite, mica, and smectite in trace amounts (<1%). The percentages of organic matter were determined by annealing at a temperature of 525 °C over 2 h.

The soil samples were processed using the procedure given in Mironov et al. (2010b). The gravimetric moisture of the soil samples, m_g, was determined as the ratio of the soil water mass, M_w, to that of the dried soil sample, M_d; that is, $m_g = M_w/M_d$. The gravimetric moisture of the samples varied from 0.03 to 0.55 g/g. A total of 10 soil samples with different moistures in this range were measured, and the temperature of each of the samples was varied from 25 °C to −30 °C. The dry soil density, ρ_d, was determined as $\rho_d = M_d/V$, where V is the volume of the coaxial container and varied from 0.72 to 0.87 g/cm^3. The measurement errors for m_g and ρ_d were estimated to be less than 6%. Similar to Mironov et al. (2010a,b), a Rohde & Schwarz ZVK vector network analyzer was used to measure the frequency spectra of the elements of the scattering matrix for the coaxial measurement container. From this measurement, the soil sample's CDC values were derived as in Mironov et al. (2010b,c). The errors varied from 3% to 30% depending on the frequency. Isothermal measurements were ensured using an SU-241 Espec heat and cold chamber, which provided temperature stability in the chamber within 0.5 °C. Unlike the measurements in Mironov et al. (2010a), ice crystallization nuclei were introduced into the soil samples to avoid depressing the soil sample's freezing temperature down to −7 °C and to ensure that the soil samples would be frozen at −1 °C.

3. Concept of a multi-relaxation spectroscopic dielectric model (MRSDM)

As in Mironov et al. (2010a), we analyze the complex dielectric constant (CDC) of moist soil, ε^*_s, in terms of the reduced complex refractive index (CRI):

$$(n^*_s - 1)/\rho_d = (\sqrt{\varepsilon^*_s} - 1)/\rho_d = (n_s - 1)/\rho_d + i\kappa_s/\rho_d, \quad (1)$$

where $n_s = Re\sqrt{\varepsilon^*_s}$ and $\kappa_s = Im\sqrt{\varepsilon^*_s}$ are the refractive index (RI) and the normalized attenuation coefficient (NAC), respectively. The NAC is considered to be a proportion of the standard attenuation coefficient to the free-space propagation constant. As observed in (1), the reduced CRI of a given substance is equal to a difference between the CRI of the substance and the CRI of air normalized by the density of the substance. For the reduced CRI of moist soil, we use the refractive mixing dielectric model as given in Mironov et al. (2010a):

$$\frac{n_s - 1}{\rho_d(m_g)} = \begin{cases} \frac{n_m-1}{\rho_m} + \frac{(n_b-1)}{\rho_b} m_g; & m_g \le m_{g1} \\ \frac{n_m-1}{\rho_m} + \frac{(n_b-1)}{\rho_b} m_{g1} + \frac{(n_t-1)}{\rho_t}(m_g - m_{g1}); & m_{g1} \le m_g \le m_{g2} \\ \frac{n_m-1}{\rho_m} + \frac{(n_b-1)}{\rho_b} m_{g1} + \frac{(n_t-1)}{\rho_t}(m_{g2} - m_{g1}) + \frac{n_{u,i}-1}{\rho_{u,i}}(m_g - m_{g2}) & m_g \ge m_{g2} \end{cases} \quad (2)$$

$$\frac{\kappa_s}{\rho_d(m_g)} = \begin{cases} \frac{\kappa_m}{\rho_m} + \frac{\kappa_b}{\rho_b} m_g; & m_g \le m_{g1} \\ \frac{\kappa_m}{\rho_m} + \frac{\kappa_b}{\rho_b} m_{g1} + \frac{\kappa_t}{\rho_t}(m_g - m_{g1}); & m_{g1} \le m_g \le m_{g2} \\ \frac{\kappa_m}{\rho_m} + \frac{\kappa_b}{\rho_b} m_{g1} + \frac{\kappa_t}{\rho_t}(m_{g2} - m_{g1}) + \frac{\kappa_{u,i}}{\rho_{u,i}}(m_g - m_{g2}) & m_g \ge m_{g2} \end{cases} \quad (3)$$

where m_{g1} and m_{g2} are the maximum gravimetric fractions of bound water and total bound water (which consists of bound water and transient bound water), respectively.

According to (2) and (3), three ranges of soil moisture, namely $m_g \leqslant m_{g1}$, $m_{g1} \leqslant m_g \leqslant m_{g2}$, and $m_g \geqslant m_{g2}$, are clearly distinguished. In the first range ($m_g \leqslant m_{g1}$), only the bound water component can form in the soil when liquid water is added to an initially dry soil. Therefore, the first range can be identified as the range of bound water. In the second range ($m_{g1} \leqslant m_g \leqslant m_{g2}$), an aggregate of both the bound and transient bound components are present; the transient bound water component forms in the soil from liquid water being added to the soil in excess of the maximum bound water fraction, m_{g1}. The second range can therefore be considered as the range of transient bound water. In the third range ($m_g \geqslant m_{g2}$), an aggregate of all three components (bound, transient bound, and unbound) of soil water are present, and only the unbound water component forms in the soil from the liquid water in excess of the maximum total bound water fraction, m_{g2}. Thus, the third range can be considered as the range of unbound water, which can exist in the form of liquid water or wet ice in thawed and frozen soil, respectively.

The maximum bound and total bound water fractions are determined at the breakpoints in the reduced CRI as a function of moisture, which occur because the reduced RIs and NACs of the bound ($(n^*_b - 1)/\rho_b$, and κ_b/ρ_b), transient bound ($(n_t - 1)/\rho_t$ and κ_t/ρ_t), and unbound ($(n_u - 1)/\rho_u$ and κ_u/ρ_u) soil water components (see Eqs. (2) and (3)) are different. The parameter m_{g1} separates the range of bound water from that of transient bound water, and m_{g2} separates the range of transient bound water from that of unbound water.

The subscripts s, d, m, b, t, u, and i, which are related to n, κ, and the density ρ, refer to the moist soil, dry soil, solid component of soil, bound water, transient bound water, unbound-liquid water, and wet ice, respectively. In addition, we assume that $\rho_b = \rho_t = \rho_u = 1$ g/cm^3 in a thawed soil and that $\rho_b = \rho_t = 1$ g/cm^3 and $\rho_i = 0.917$ g/cm^3 in a frozen soil. This assumption is applied to the densities of the soil water components only in the framework of the proposed soil dielectric model and will be confirmed when the dielectric model is validated as a whole.

According to (1), the RI, n_p, and NAC, κ_p, with the subscript p, which indicate the bound ($p = b$), transient bound ($p = t$), unbound-liquid ($p = u$), and wet ice ($p = i$) soil water components, can be expressed through the dielectric constant (DC), ε_p', and the loss factor (LF), ε_p'', as follows:

$$n_p\sqrt{2} = \sqrt{\sqrt{(\varepsilon_p')^2 + (\varepsilon_p'')^2} + \varepsilon_p'}, \qquad \kappa_p\sqrt{2} = \sqrt{\sqrt{(\varepsilon_p')^2 + (\varepsilon_p'')^2} - \varepsilon_p'}. \tag{4}$$

Similar to Mironov et al. (2013b), we express the dielectric constant and the loss factor of the components of soil water in (4) using the equations for the Debye multiple relaxations (Kremer et al., 2002) of non-conductive liquids, which account for only bias electric currents:

$$\begin{aligned} \varepsilon_p' &= \frac{\varepsilon_{0pL}-\varepsilon_{0pM}}{1+(2\pi f\tau_{pL})^2} + \frac{\varepsilon_{0pM}-\varepsilon_{0pH}}{1+(2\pi f\tau_{pM})^2} + \frac{\varepsilon_{0pH}-\varepsilon_{\infty pH}}{1+(2\pi f\tau_{pH})^2} + \varepsilon_{\infty pH}, \\ \varepsilon_p'' &= \frac{\varepsilon_{0pL}-\varepsilon_{0pM}}{1+(2\pi f\tau_{pL})^2} 2\pi f\tau_{pL} + \frac{\varepsilon_{0pM}-\varepsilon_{0pH}}{1+(2\pi f\tau_{pM})^2} 2\pi f\tau_{pM} + \frac{\varepsilon_{0pH}-\varepsilon_{\infty pH}}{1+(2\pi f\tau_{pH})^2} 2\pi f\tau_{pH}, \end{aligned} \tag{5}$$

where f is the wave frequency, ε_{0pL}, ε_{0pM}, and ε_{0pH} are the low frequency limits of the dielectric constants that correspond to the respective relaxations, and $\varepsilon_{\infty pH}$ is a high frequency limit for the dielectric constant of the dipole relaxation. The subscripts H, M, and L refer to the high frequency, middle frequency, and low frequency relaxations, respectively. The high frequency relaxation is a dipole relaxation, whereas the middle frequency and low frequency relaxations are assumed to be the interfacial (Maxwell–Wagner) relaxations that arise due to periodic recharge of soil water layers under the influence of an alternating electromagnetic field. The parameters τ_{pL}, τ_{pM}, and τ_{pH} are the times of the respective relaxations. All of these parameters should be related to the bound ($p = b$), transient bound ($p = t$), unbound-liquid ($p = u$), and wet ice ($p = i$) components of the soil water. In the case of bound water, a three relaxation form of Eq. (5) is used. In the case of transient bound water, a two relaxation equation is applied, which follows from (5) with $\varepsilon_{0tL} = \varepsilon_{0tM}$. In the case of unbound water, a single relaxation equation is used, which follows from (5) with $\varepsilon_{0uL} = \varepsilon_{0uM} = \varepsilon_{0uH}$.

The LFs, ε''_p, that are determined by Eq. (5) do not include a term that accounts for the ohmic conductivity of the soil water components. Nevertheless, keeping in mind that only the bias currents account for the DC of moist soil, ε'_s, we can express this value in the form

$$\varepsilon_s' = n_s^2 - \kappa_s^2, \tag{6}$$

where Eqs. (2)–(4) are used to calculate the RI, n_s, and the NAC, κ_s.

At the same time, the LF of moist soil, ε''_s, can be represented as the sum of two terms that account for the bias currents, ε''_{sb}, and the conductivity currents, ε''_{sc}, that run through the moist sample. The terms that account for the bias and ohmic conductivity currents can be expressed as $\varepsilon''_{sb} = 2n_s\kappa$ and $\varepsilon''_{sc} = \sigma_s/2\pi f\varepsilon_r$, respectively. Here, n_s and κ_s are calculated from (4) and (5), σ_s is the specific conductivity of the moist soil, and $\varepsilon_r = 8.854$ pF/m is the dielectric constant of the free space. We now represent the specific electrical conductivity of the moist soil, σ_s, as the sum of the specific conductivities, σ_p, of all of the components of soil water ($p = b$, t, u, i), which are weighted by their relative volumetric fractions, W_p; that is, $\sigma_{sc} = W_b\sigma + W_t\sigma + W_{u,i}\sigma_{u,i}$. By definition, the volumetric fraction, W_p ($p = b$, t, u, i), is expressed as $W_p = V_p/V$, where V is the sample volume, and V_p is the volume of water in the soil that relates to a specific component p. V and V_p can be expressed through the respective masses and densities as $V = M_d/\rho_d$ and $V_p = M_p/\rho_p$. Consequently, the volumetric fraction W_p can be expressed in the form $W_p = m_{g,p}(\rho_d/\rho_p)$, where $m_{g,p}$ is the gravimetric moisture that relates to a specific soil water component p. As a result, the expression for the LF of moist soil can be written as:

$$\varepsilon_s'' = \begin{cases} 2n_s\kappa_s + \rho_d(m_g)(m_g/\rho_b)\sigma_b/2\pi f\varepsilon_r, & 0 \le m_g \le m_{g1}; \\ 2n_s\kappa_s + \rho_d(m_g)[(m_{g1}/\rho_b)\sigma_b + [(m_g - m_{g1})/(\rho_t)]\sigma_t]/2\pi f\varepsilon_r, & m_{g1} \le m_g \le m_{g2}; \\ 2n_s\kappa_s + \rho_d(m_g)[(m_{g1}/\rho_b)\sigma_b + [(m_{g2} - m_{g1})/(\rho_t)]\sigma_t + [(m_g - m_{g2})/\rho_{u,i}]\sigma_{u,i}]/2\pi f\varepsilon_r, & m_g \ge m_{g2}. \end{cases} \tag{7}$$

Eqs. (1)–(7) show that the DC and LF spectra at a given soil temperature as a function of the input variables (dry soil density, ρ_d, gravimetric soil moisture m_g, and wave frequency f) can be calculated using the following set of parameters: $(n_m - 1)/\rho_m$, κ_m/ρ_m, m_{g1}, m_{g2}, ε_{0pQ}, $\varepsilon_{\infty pH}$, τ_{pQ}, σ_p, which are related to i) the bound ($p = b$), transient bound ($p = t$), unbound-liquid ($p = u$), and wet ice ($p = i$) components of the soil water and ii) the high frequency ($Q = H$), middle frequency ($Q = M$), and low frequency ($Q = L$) relaxations of the soil water components. These parameters can be regarded as characteristics of the MRSDM. The reduced RI, $(n_m - 1)/\rho_m$, and the NAC, κ_m/ρ_m, are mineralogical characteristics of the soil solids. The maximum gravimetric fractions of the bound water, m_{g1}, and of the total bound water, m_{g2}, are hydrological characteristics of the bulk soil. The low limit and high limit dielectric constants, ε_{0pQ} and $\varepsilon_{\infty pH}$, in conjunction with the values of the relaxation time, τ_{pQ}, are relaxation characteristics of the soil water molecules. Finally, the conductivities, σ_p, are electrical characteristics of the soil water solutions. These parameters should vary with temperature. In the next section, we outline the methodology for retrieving all of the parameters of the multi-relaxation spectroscopic dielectric model.

4. Retrieving the parameters of the multi-relaxation spectroscopic dielectric model

Laboratory measurements of the CDC spectra were used to retrieve the parameters of the multi-relaxation dielectric model of moist soil. The measured reduced RI and NAC are shown in Fig. 1 with the results of fitting the theoretical models (2) and (3) to the measured data. The measured RI and NAC can be calculated using Eq. (1) and the data shown in Fig. 1 and Table 1.

The results in Fig. 1 show that models (2) and (3) are satisfactory. The RI and NAC measurements are piecewise linear in certain moisture ranges, which indicates the contributions of the particular components of water. The maximum fractions m_{g1} and m_{g2} are determined as the transition points from one linear segment of the fit to another (Fig. 1). These values were retrieved by fitting the theoretical models (2) and (3) to the measured reduced RI and NAC values as a function of soil moisture at various temperatures. Thus, the obtained maximum fractions m_{g1} and m_{g2} depend on the temperature, particularly in the case of frozen soil samples. These dependences were fitted with polynomials and exponential functions and yielded the following equations:

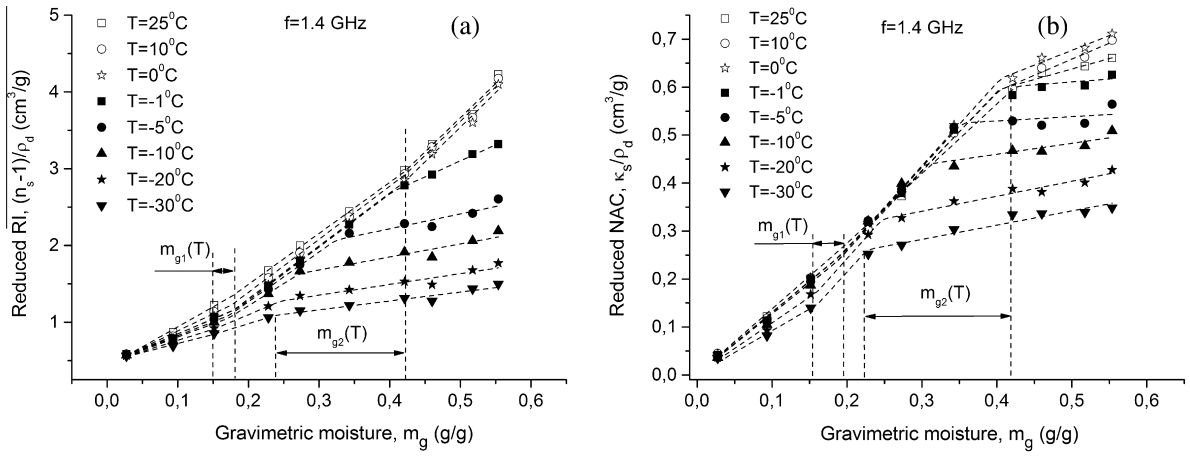

Fig. 1. Behavior of the reduced characteristics for (a) the RI, $(n_s-1)/\rho_d$, and (b) NAC, $(\kappa_s-1)/\rho_d$, vs. gravimetric moisture at a fixed frequency of 1.4 GHz at temperatures from 25 °C to −30 °C. The dashed lines indicate fits of Eqs. (2) and (3) to the measured data.

Table 1
The values of gravimetric moistures and dry soil densities observed in measurements.

m_g (g/g)	0.027	0.093	0.152	0.228	0.273	0.343	0.400	0.460	0.517	0.554
ρ_d (g/cm^3)	0.87	0.808	0.767	0.747	0.752	0.758	0.809	0.748	0.715	0.774

$$
\begin{aligned}
&m_{g1} = 0.19 - 0.00037T, \qquad 0\ ^\circ\mathrm{C} \le T \le 25\ ^\circ\mathrm{C};\\
&m_{g1} = 0.114 + 0.081\exp(T/50.6), \qquad -30\ ^\circ\mathrm{C} \le T \le -1\ ^\circ\mathrm{C};\\
&m_{g2} = 0.404, \qquad 0\ ^\circ\mathrm{C} \le T \le 25\ ^\circ\mathrm{C};\\
&m_{g2} = 0.237 + 0.225\exp(T/4.81), \qquad -30\ ^\circ\mathrm{C} \le T \le 1\ ^\circ\mathrm{C}.
\end{aligned}
\tag{8}
$$

By fitting the theoretical models (2) and (3) to the reduced RI and NAC measurements as a function of soil moisture at various temperatures (Fig. 1), the values of $(n_m-1)/\rho_m$ and κ_m/ρ_m were retrieved. The latter are equal to the values of $(n_s-1)/\rho_d$ and κ_s/ρ_d in the fitted models (2) and (3) at $m_g = 0$, respectively. Thus, the obtained temperature dependences for the values of the reduced RI, $(n_m-1)/\rho_m$, and the NAC, κ_m/ρ_m, that characterize the soil solids were fitted with polynomials and yielded the following equations:

$$
\begin{aligned}
&(n_m-1)/\rho_m = 0.467 - 0.001T, \qquad -30\ ^\circ\mathrm{C} \le T \le 25\ ^\circ\mathrm{C};\\
&\kappa_m/\rho_m = 0.0015, \qquad -30\ ^\circ\mathrm{C} \le T \le 25\ ^\circ\mathrm{C}.
\end{aligned}
\tag{9}
$$

With the data shown in Fig. 1 and Eqs. (1) and (2), the values of the RI of unbound water are calculated as $n_u = 10$ and $n_i = 5.6$ at temperatures of 0 °C and −1 °C, respectively, and n_i sharply decreases to 2.4 at −30 °C. The latter value is similar to the value of 1.77 for crystal ice. Therefore, we conditionally assume that the soil samples are in a frozen state in the temperature range $-30\ ^\circ\mathrm{C} \leqslant T \leqslant -1\ ^\circ\mathrm{C}$. It is worth noting that this assumption is applied in the methodology that is used to analyze the measured dielectric data.

Now that the dependence of the complex refractive index on moisture has been established and the division between the frozen and thawed states has been clarified, we turn our attention to the methodology for retrieving the spectral parameters in Eqs. (5) and (6). The spectra for the DC and LF of moist soil samples measured at different moistures and temperatures will be used to determine these parameters. Fig. 2 shows several patterns of these spectra for the thawed and frozen soil samples. As can be deduced from

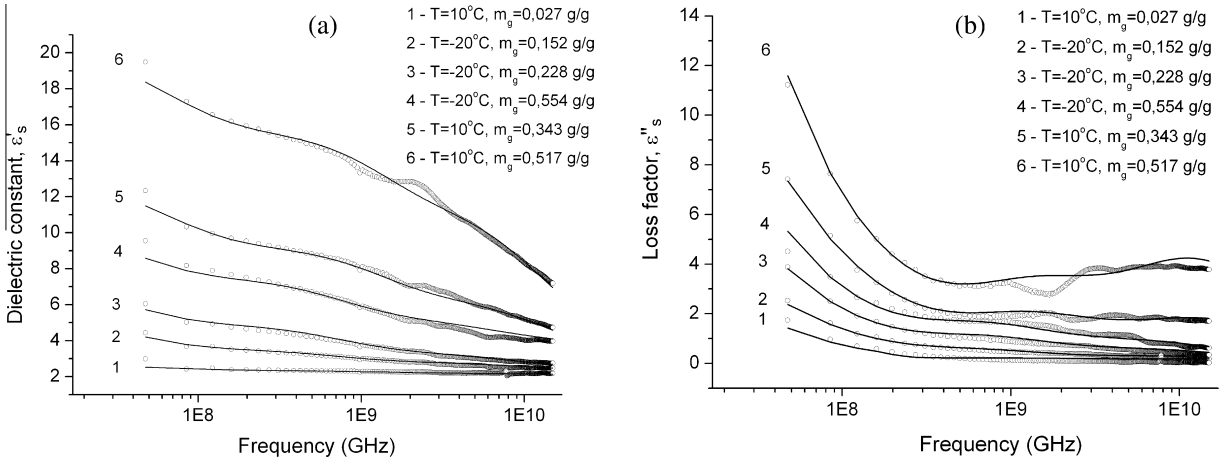

Fig. 2. Spectra of (a) dielectric constant, ε_s', and (b) loss factor, ε_s'', from measured data (symbols) and fitted (lines) with (i) formulas (6), (2), (3), (8), (9), (4) and (5) and (ii) formulas (7), (2), (3), (8), (9), (4) and (5), respectively. The data represent both thawed (T = 10 °C) and frozen (T = −20 °C) soils that contain only bound water (m_g = 0.027 and m_g = 0.152), bound water and transient bound water (m_g = 0.228 and m_g = 0.343), and bound water, transient bound water and unbound-liquid water at T = 10 °C or wet ice at T = −20 °C (m_g = 0.517 and m_g = 0.554).

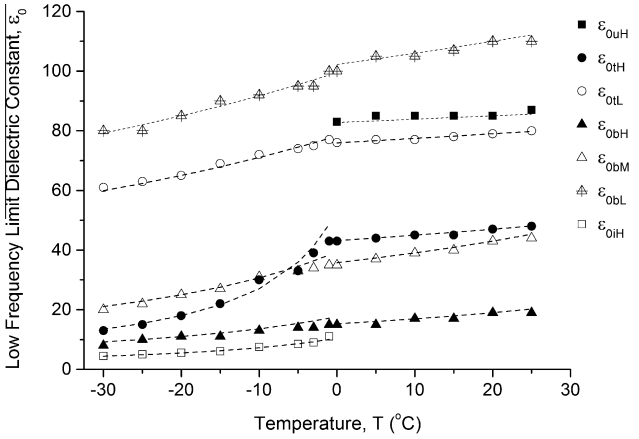

Fig. 3. Low frequency limit dielectric constants as a function of temperature. The measured data and respective fits are shown with symbols and lines, respectively, for the bound water, ε_{0bQ}, transient bound water, ε_{0tQ}, unbound-liquid water, ε_{0uQ}, and wet ice, ε_{0iQ}, at high frequency ($Q = H$), middle frequency ($Q = M$), and low frequency ($Q = L$) relaxations.

the equations in (8), the samples shown in Fig. 2 contain bound water (plots 1 and 2), bound water and transient bound water (plots 3 and 5), and all three soil water components (plots 4 and 6). In this case, the frozen soil samples contain unbound soil water in the form of wet ice.

In the first phase of fitting, the DC spectra of the samples are fitted using only the measured values of soil moisture in the range $0 < m_g < m_{g1}$ so that only the bound water component is contained in the samples. The theoretical model of the soil DC that is fitted to the measured spectra is calculated by applying Eqs. (6), (2), (3), (8), (9), (4) and (5).

The theoretical spectra that are calculated with Eqs. (6), (2), (3), (8), (9), (4) and (5) and account for (i) only high frequency relaxation, (ii) high frequency and middle frequency relaxations, and (iii) high frequency, middle frequency and low frequency relaxations are successively fitted to the measured data and yield the following sets of spectroscopic parameters, respectively: (i) ε_{0bH} and τ_{bH}; (ii) ε_{0bH}, τ_{bH}, ε_{0bM}, and τ_{bM}, and (iii) ε_{0bH}, τ_{bH}, ε_{0bM}, τ_{bM}, ε_{0bL}, and τ_{bL}. The high frequency limit $\varepsilon_{\infty pH}$, $p = b, t, u, i$, is assigned a value of 4.9 from this point on. Figs. 3 and 4 show the spectroscopic parameters that are obtained for the bound water

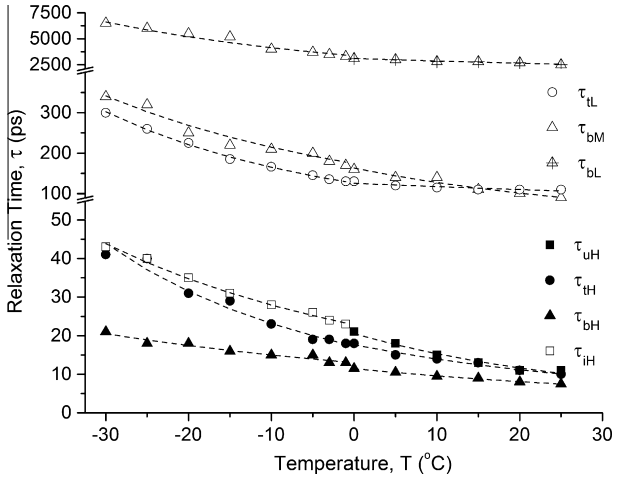

Fig. 4. Relaxation time as a function of temperature. The measured data and respective fits are shown with symbols and lines, respectively, for the bound water, τ_{bQ}, transient bound water, τ_{tQ}, unbound-liquid water, and wet ice, τ_{iQ}, at high frequency ($Q = H$), middle frequency ($Q = M$), and low frequency ($Q = L$) relaxations.

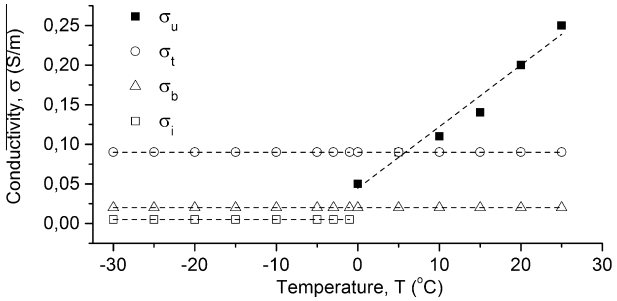

Fig. 5. Conductivity as a function of temperature. The measured data and their fits are shown with symbols and lines, respectively, for the bound water, σ_b, transient bound water, σ_t, unbound-liquid water, σ_u, and wet ice, σ_i.

component as a function of temperature. The theoretical spectra for the dielectric constant calculated at the derived values of the parameters ε_{0bH}, τ_{bH}, ε_{0bM}, τ_{bM}, ε_{0bL}, τ_{bL}, are also shown in Fig. 2 and demonstrate good correlations with the measured data.

After all of the spectroscopic parameters for the bound soil water (ε_{0bH}, τ_{bH}, ε_{0bM}, τ_{bM}, ε_{0bL}, and τ_{bL}) were derived using only the dielectric constant spectra that were measured for moist soil samples, we can perform further fitting to obtain the specific conductivity of the bound soil water from the loss factor spectra measured for gravimetric soil moistures in the range $0 < m_g < m_{g1}$. To calculate the theoretical values of the loss factor, we apply Eqs. (7), (2), (3), (8), (9), (4) and (5) using the values of the spectroscopic parameters that were previously derived. The fitted theoretical model for the loss factor calculated using the derived values of ε_{0bH}, τ_{bH}, ε_{0bM}, τ_{bM}, ε_{0bL}, τ_{bL}, and σ_b is also shown in Fig. 2 and shows a good correlation with the measured data. As a result of this fitting, the value of the specific conductivity for the bound soil water, σ_b, was obtained as a function of temperature and is shown in Fig. 5.

The spectra measured for the samples that contain both bound water and transient bound water components were used in the second phase of fitting, and the same fitting approach was applied with the values of the parameters ε_{0bH}, τ_{bH}, ε_{0bM}, τ_{bM}, ε_{0bL}, τ_{bL} and σ_b from the first phase of fitting. The results of the second phase of fitting for the derived values ε_{0tH}, τ_{tH}, ε_{0tL}, τ_{tL}, and σ_t are shown in Figs. 3–5.

The third phase of fitting used the spectra that were measured for the samples that contain all three components of soil water using the values of the parameters ε_{0bH}, τ_{bH}, ε_{0bM}, τ_{bM}, ε_{0bL}, τ_{bL}, σ_b, ε_{0tH}, τ_{tH}, ε_{0tL}, τ_{tL}, and σ_t from the first and second phases of fitting. The results of the third phase of fitting for the derived values of $\varepsilon_{0u,iH}$, $\tau_{u,iH}$, and $\sigma_{u,i}$ are shown in Figs. 3–5. Now that the temperature dependences of all of the spectroscopic parameters and specific conductivities have been obtained, we will consider the temperature-dependent multi-relaxation spectral dielectric model (TD MRSDM) for moist soil following the methodology of Mironov et al. (2010a), which outlined only a single relaxation case.

5. The temperature-dependent multi-relaxation spectroscopic dielectric model (TD MRSDM)

We suggest that the temperature dependences for the low frequency limit dielectric constants observed in Fig. 3 follow the equation that was obtained in Mironov et al. (2010a) with the use of the Clausius–Mossotti law (Dorf, 1997):

$$\varepsilon_{0pQ}(T) = \frac{1 + 2\exp[F_{pQ}(T_{s\varepsilon pQ}) - \beta_{vpQ}(T - T_{s\varepsilon pQ})]}{1 - \exp[F_{pQ}(T_{s\varepsilon pQ}) - \beta_{vpQ}(T - T_{s\varepsilon pQ})]}, \qquad F_{pQ}(T) = \ln\left[\frac{\varepsilon_{0pQ}(T) - 1}{\varepsilon_{0qQ}(T) + 2}\right], \tag{10}$$

Table 2
(a) and (b) TD MRSDM parameters for all components of soil water in the temperature range $-30\ ^\circ C \leqslant T \leqslant +25\ ^\circ C$.

Soil water component		Bound soil water, $p = b$					
Relaxation		High frequency		Middle frequency		Low frequency	
Temperature range (a)		$T \leqslant -1\ ^\circ C$	$T \geqslant 0\ ^\circ C$	$T \leqslant -1\ ^\circ C$	$T \geqslant 0\ ^\circ C$	$T \leqslant -1\ ^\circ C$	$T \geqslant 0\ ^\circ C$
Parameter	Units						
$\varepsilon_{0p}(T_{s\varepsilon 0p})$	–	11	19	25	43	85	110
β_{v0p}	1/K	3.73×10^{-3}	1.54×10^{-3}	1.91×10^{-3}	6.39×10^{-4}	2.47×10^{-4}	9.94×10^{-5}
$T_{s\varepsilon 0p}$	°C	−20	20	−20	20	−20	20
$\Delta H_p/R$	K	751	1113	1231	1630	1240	361
$\Delta S_p/R$	–	−1.55	−0.1	−2.39	−0.86	−5.32	−8.46
Temperature range		$T \leqslant -1\ ^\circ C$			$T \geqslant 0\ ^\circ C$		
$\sigma_p(T_{s\sigma p})$	S/m	0.02			0.02		
$\beta_{\sigma p}$	(S/m)/K	0			0		
$T_{s\sigma p}$	°C	−20			20		

Soil water component		Transient bound water ($p = t$)				Wet ice water ($p = i$)	Unbound-liquid water ($p = u$)
Relaxation		High frequency		Low frequency		High frequency	High frequency
Temperature range (b)		$T \leqslant -1\ ^\circ C$	$T \geqslant 0\ ^\circ C$	$T \leqslant -1\ ^\circ C$	$T \geqslant 0\ ^\circ C$	$T \leqslant -1\ ^\circ C$	$T \geqslant 0\ ^\circ C$
Parameter	Units						
$\varepsilon_{0p}(T_{s\varepsilon 0p})$	–	18	47	65	79	5.5	85
β_{v0p}	1/K	4.64×10^{-3}	2.59×10^{-4}	3.69×10^{-4}	7.24×10^{-5}	9.04×10^{-3}	4.53×10^{-5}
$T_{s\varepsilon 0p}$	°C	−20	20	−20	20	−20	20
$\Delta H_p/R$	K	1792	1548	1679	251	1185	1979
$\Delta S_p/R$	–	1.97	1.06	−0.42	−5.65	−0.53	2.49
Temperature range		$T \leqslant -1\ ^\circ C$		$T \geqslant 0\ ^\circ C$		$T \leqslant -1\ ^\circ C$	$T \geqslant 0\ ^\circ C$
$\sigma_p(T_{s\sigma p})$	S/m	0.05		0.05		5×10^{-3}	0.2
$\beta_{\sigma p}$	(S/m)/K	0		0		0	7.77×10^{-3}
$T_{s\sigma p}$	°C	−20		20		−20	20

where ε_{0pQ} and β_{vpQ} are the low frequency limit dielectric constants and the volumetric expansion coefficients, respectively, that are related to the bound water ($p = b$), transient bound water ($p = t$), unbound-liquid water ($p = u$), and wet ice ($p = i$) components of the soil water, the subscript Q represents the low ($Q = L$), middle ($Q = M$), and high ($Q = H$) frequency relaxations of the soil water components, and $T_{s\varepsilon pQ}$ represents the starting temperature, which can be any value from the measured temperature intervals. The values of β_{vpQ} and $\varepsilon_{0pQ}(T_{s\varepsilon pQ})$ can be determined by fitting the theoretical model (10) to the measured data shown in Fig. 3. The fitted theoretical models for the low frequency limit dielectric constants that were calculated with the values of β_{vpQ} and $\varepsilon_{0pQ}(T_{s\varepsilon pQ})$ from the fitting are also shown in Fig. 3 and agree well with the measured data. This fitting is performed separately for the thawed and frozen soil samples. The values of β_{vpQ}, $T_{s\varepsilon pQ}$, and $\varepsilon_{0pQ}(T_{s\varepsilon pQ})$ derived from the fitting are given in Table 2(a) and (b).

The relaxation time also requires a temperature dependence and is shown as a function of temperature in Fig. 4. The measured relaxation time can be described by the Eyring equation (Dorf, 1997):

$$\ln\left(\frac{kT_K}{h}\tau_{pQ}\right) = \frac{\Delta H_{pQ}}{R}\frac{1}{T_K} - \frac{\Delta S_{pQ}}{R}, \tag{11}$$

where h is the Plank constant (6.624×10^{-34} Js), k is the Boltzmann constant (1.38×10^{-23} J K^{-1}), ΔH_{pQ} is the activation energy of the relaxation process, R is the universal gas constant (8.314×10^{3} J K^{-1} kmol^{-1}), ΔS_{pQ} is the entropy of activation, and T_K is the temperature in Kelvin. The ratios $\Delta H_{pQ}/R$ and $\Delta S_{pQ}/R$, which are proportional to the activation energy and the entropy of activation, respectively, can be determined by linear fitting the measured value of $\ln(kT_K\tau/h)$ to $1/T_K$ as shown in Fig. 4. The calculated values of $\Delta H_{pQ}/R$ and $\Delta S_{pQ}/R$ are given in Table 2(a) and (b) and can be used to calculate the relaxation time using Eq. (11). The theoretical models for the relaxation times that were calculated with the values of $\Delta H_{pQ}/R$ and $\Delta S_{pQ}/R$ from the fitting are also shown in Fig. 4 and show good agreement with the measured data.

Finally, we suggest that the conductivity, σ_p, has a linear dependence with temperature as is characteristic of ionic solutions:

$$\sigma_p(T) = \sigma_p(T_{s\sigma p}) + \beta_{\sigma p}(T - T_{s\sigma p}), \tag{12}$$

where $\beta_{\sigma p}$ is the derivative of conductivity with respect to temperature, which is also called the conductivity temperature coefficient, and $\sigma_p(T_{s\sigma p})$ is the value of conductivity at an arbitrary starting temperature, $T_{s\sigma p}$, that is taken from the measured range.

The values of σ_p and $\beta_{\sigma p}$ can be determined by fitting the theoretical model (12) to the measured data shown in Fig. 5. This fitting was performed separately for the thawed and frozen soil samples. The theoretical models for the conductivity that were calculated with the values of σ_p and $\beta_{\sigma p}$ from the fitting are also shown in Fig. 5 and agree well with the measured data. The values of σ_p and $\beta_{\sigma p}$ that are derived from the fitting are given in Table 2(a) and (b).

As a result of the analyses conducted in this section, the TD MRSDM can be defined by the following steps, which form the algorithm procedure.

1. The temperature, T, must be assigned in cases of thawed or frozen soil.
2. The values of the Debye parameters, including the low frequency limit, relaxation time, and conductivity, for all types of soil water are calculated with Eqs. (10)–(12) and the data in Table 2(a) and (b).
3. Once the values of $\varepsilon_{0pQ}(T)$, $\tau_{pQ}(T)$, and $\sigma_p(T)$ are known, the values of the dielectric constant, $\varepsilon'_p(f, T)$, and the loss factor $\varepsilon''_p(f, T)$ for all components of the soil water can be calculated as a function of frequency at a given temperature using the equations in (5).

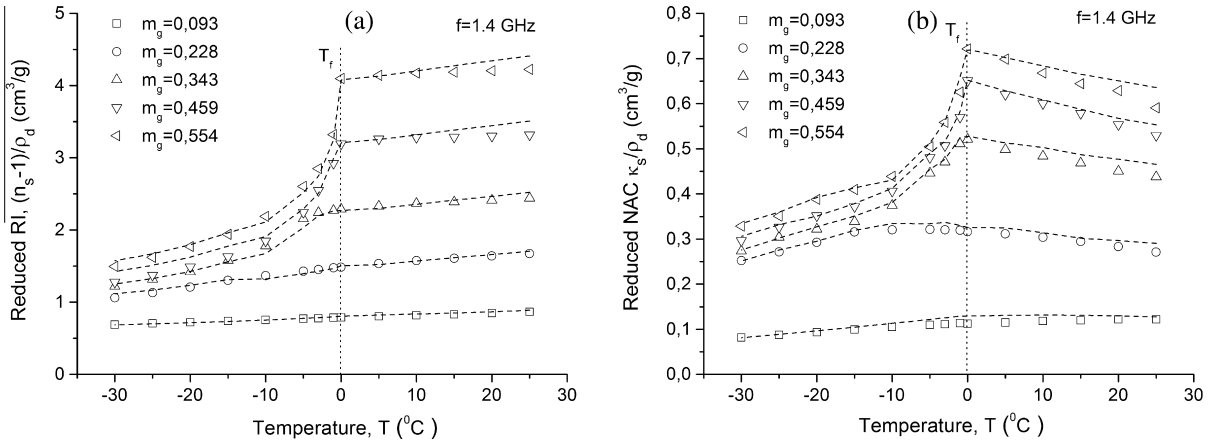

Fig. 6. Behavior of the reduced (a) RI, $(n_s - 1)/\rho_d$, and (b) NAC, κ_s/ρ_d, vs. temperature with varying values of gravimetric moisture at a frequency of 1.4 GHz. The measured and predicted data are shown with symbols and dashed lines, respectively.

4. The values of $\varepsilon'_p(f, T)$ and $\varepsilon''_p(f, T)$ are translated to the RI, n_p, and the NAC, κ_p, for all of the components of the soil water using the equations in (4).
5. The gravimetric soil moisture, m_g, and the dry soil bulk density, ρ_d, must be assigned, and Eqs. (2), (3), (8) and (9) are applied to calculate the soil RI, $n_s(\rho_d, m_g, f, T)$, and the NAC, $\kappa_s(\rho_d, m_g, f, T)$ accounting for bias currents.
6. Finally, the values of $n_s(\rho_d, m_g, f, T)$ and $\kappa_s(\rho_d, m_g, f, T)$ are translated to the soil dielectric constant, $\varepsilon'_s(\rho_d, m_g, f, T)$, and the loss factor, $\varepsilon''_s(\rho_d, m_g, f, T)$, with Eqs. (6)–(8), respectively, using the values of the specific conductivities from Table 2(a) and (b).

In the following section, the TD MRSDM that was developed for an organic soil will be evaluated in terms of the prediction error by correlating the predicted moist soil dielectric data with measured data in the multidimensional domain of dry soil density, temperature, frequency, and moisture.

6. Evaluation of the TD MRSDM

Fig. 6 shows the values predicted with the TD MRSDM and the values measured at a frequency of 1.4 GHz as a function of temperature for samples with varying moistures and dry soil densities. The predicted and measured values agree well with each other. To estimate the deviations of the predicted CDC values from the measured values across the entire range of measured dry densities, moistures, temperatures, and frequencies, we calculated the coefficient of determination for the DC, $R^2_{\varepsilon'}$, and the LF, $R^2_{\varepsilon''}$. Their values were found to be $R^2_{\varepsilon'} = 0.997$ and $R^2_{\varepsilon''} = 0.991$. The RMSEs of the predicted values relative to the measured values were $RMSE_{\varepsilon'} = 0.348$ and $RMSE_{\varepsilon''} = 0.188$ for the DC and LF, respectively.

7. Conclusions

A temperature-dependent multi-relaxation spectroscopic dielectric model was developed for an organic-rich soil that was collected from a grassy moss tundra site located on the Yamal Peninsula, Russian Federation. The model is presented as an ensemble of analytical expressions and gives the complex dielectric constants of the thawed and frozen soil using the dry soil density, gravimetric moisture, temperature, and wave frequency as input variables. The validation of this model demonstrates good agreement with the measured data for frequencies from 0.05 to 15 GHz, gravimetric moistures from 0.03 to 0.55 g/g, and temperatures from −30 °C to +25 °C with dry soil densities of 0.72 to 0.87 g/cm^3. With such wide variations of all of the input variables, the coefficients of determination for the dielectric constant, $R^2_{\varepsilon'}$, and the loss factor, $R^2_{\varepsilon''}$ were found to be $R^2_{\varepsilon'} = 0.997$ and $R^2_{\varepsilon''} = 0.991$. The RMSEs of the predicted values of the dielectric constant and the loss factor relative to the measured values were $RMSE_{\varepsilon'} = 0.348$ and $RMSE_{\varepsilon''} = 0.188$, respectively.

These error estimates are less than those in the model of Mironov and Fomin (2009), which is successfully used in the operational algorithm of SMOS to retrieve soil moisture (Mialon et al., 2015). Therefore, the model is acceptable for practical use to develop remote sensing algorithms that are pertinent to the Arctic regions provided that the topsoil of the area being analyzed is predominantly composed of organic soil. Although this model is entirely based on laboratory experiments, it can consider the full range of observed soil moistures and temperatures. Nevertheless, in real environmental conditions, a more general soil dielectric model that also accounts for a wide variety of organic, mineral and mixed composition Arctic soil types is needed. The model proposed in this study will be a component of such a generalized dielectric model. Generalized dielectric models that are applicable to a variety of thawed mineral soils present in the natural environment of temperate zones have been developed (Dobson et al., 1985; Mironov and Fomin, 2009), and their applicability for use in moisture retrieval algorithms under real environmental conditions was recently confirmed (Mialon et al., 2015).

A major advantage of the proposed dielectric model compared to the previous single-relaxation model of Mironov et al. (2010a) is that it covers a wider frequency band of 0.05–15 GHz instead of 1 to 16 GHz, which was made possible by taking into account multiple relaxations of the different soil water components. In addition, a realistic soil freezing temperature of −1 °C was attained in a freezing run instead of a depressed soil freezing temperature of −7 °C that was inherent to the model of Mironov et al. (2010a).

This model forms the basis for developing data processing algorithms for modern remote sensing missions, such as AQUA, GCOM-W, SMOS, SMAP, RADARSAT, and ALOS PALSAR, as well as for perspective P-band sensors, for which the depth of sensing is expected to increase. In addition, it facilitates the application of GPR and TDR instruments, which operate in the megahertz band, to interpret the results of in situ measurements of the active permafrost layer, including studies of freeze/thaw processes.

Conflict of interest

There is no conflict of interest.

Acknowledgment

The study was supported by the Russian Science Foundation (project 14-17-00656).

References

Bircher, S., Balling, J.E., Skou, N., Kerr, Y.H., 2012. Validation of SMOS brightness temperatures during the HOBE airborne campaign, western Denmark. IEEE Trans. Geosci. Remote Sens. 50, 1468–1482.

Dobson, M.C., Ulaby, F.T., Hallikainen, M.T., El-Rayes, M.A., 1985. Microwave dielectric behavior of wet soil. Part II: Dielectric mixing models. IEEE Trans. Geosci. Remote Sens. 23, 35–45.

Dorf, R.C. (Ed.), 1997. Electrical Engineering Handbook, second ed. CRC Press, Boca Raton, FL.

Jones, L.A., Kimball, J.S., McDonald, K.C., Chan, S.T.K., Njoku, E.G., Oechel, W.C., 2007. Satellite microwave remote sensing of boreal and arctic soil temperatures from AMSR-E. IEEE Trans. Geosci. Remote Sens. 45, 2004–2018.

Kremer, F., Schonhals, A., Luck, W., 2002. Broadband Dielectric Spectroscopy, New York.

Mialon, A., Richaume, P., Leroux, D., Bircher, S., Al, Bitar A., Pellarin, T., Wigneron, J.-P., Yann, H., Kerr, Y.H., 2015. Comparison of Dobson and Mironov dielectric models in the SMOS soil moisture retrieval algorithm. IEEE Trans. Geosci. Remote Sens., 53

Mironov, V.L., Fomin, S.V., 2009. Temperature and mineralogy dependable model for microwave dielectric spectra of moist soils. PIERS Online 5, 411–415.

Mironov, V.L., De Roo, R.D., Savin, I.V., 2010a. Temperature-dependable microwave dielectric model for an arctic soil. IEEE Trans. Geosci. Remote Sens. 48, 2544–2556.

Mironov, V.L., Komarov, S.A., Lukin, Yu.I., Shatov, D.S., 2010b. A technique for measuring the frequency spectrum of the complex permittivity of soil. J. Commun. Technol. Electron. 55, 1368–1373.

Mironov, V.L., Muzalevskiy, K.V., Savin, I.V., 2013a. Retrieving temperature gradient in frozen active layer of arctic tundra soils from radiothermal observations in L - Band—theoretical modeling. IEEE J. Sel. Topics Appl. Earth Observ. Remote Sens. 6, 1781–1785.

Mironov, V.L., Bobrov, P.P., Fomin, S.V., Karavaiskii, A.Yu., 2013b. Generalized refractive mixing dielectric model of moist soils considering ionic relaxation of soil water. Russ. Phys. J. 56, 319–324.

Mironov, V.L., Molostov, I.P., Lukin, Yu.I., Karavaisky, A. Yu., 2013c. Method of retrieving permittivity from S12 element of the waveguide scattering matrix. International Siberian Conference on Control and Communications (SIBCON), pp. 1–3. doi:http://dx.doi.org/10.1109/SIBCON.2013.6693609 (IEEE Conference Publications).

Rautiainen, K., Lemmetyinen, J., Pulliainen, J., Vehvilainen, J., Drusch, M., Kontu, A., Kainulainen, J., Seppanen, J., 2012. L-band radiometer observations of soil processes in boreal and subarctic environments. IEEE Trans. Geosci. Remote Sens. 50, 1483–1497.

Watanabe, M., Kadosaki, G., Kim, Yongwon., Ishikawa, M., Kushida, K., Sawada, Y., Tadono, T., Fukuda, M., Sato, M., 2012. Analysis of the sources of variation in L-band backscatter from terrains with permafrost. IEEE Trans. Geosci. Remote Sens. 50, 44–54.